International Journal of Design & Nature and Ecodynamics
Vol. 21, No. 10, October, 2026, pp. 3125-3139
Journal homepage: http://iieta.org/journals/ijdne

Seasonal Patterns and Spatial Extent of Surface Urban Heat Islands Across a Climatic Gradient in Iraq: A Landsat 9 Comparison of Mosul, Baghdad, and Basra

Omar A. Hammad[1*], Natheer S. Hamad[1], Ahmed M. El Kenawy[2]

[1] Department of Geography, College of Education for Humanities, University of Anbar, Ramadi 55431, Iraq
[2] Department of Geography, Mansoura University, Mansoura 35516, Egypt

Corresponding Author Email: ome24h5003@uoanbar.edu.iq

Copyright: ©2026 The authors. This article is published by IIETA and is licensed under the CC BY 4.0 license (http://creativecommons.org/licenses/by/4.0/).

https://doi.org/10.18280/ijdne.211022

Received: 14 August 2026
Revised: 18 October 2026
Accepted: 25 October 2026
Available online: 31 October 2026

Keywords:
surface urban heat island, land surface temperature, surface urban heat island intensity, spatial distribution, seasonal variation

ABSTRACT

Surface urban heat islands (SUHIs) reflect the effects of urbanization on local thermal patterns. This study comparatively examined their peak intensity, spatial extent, and seasonal persistence in Mosul, Baghdad, and Basra, Iraq, during 2025, using Landsat imagery. A total of 12 Landsat 9 satellite scenes were analyzed, comprising four scenes per city, with one scene representing each season of 2025. Land surface temperature (LST), surface urban heat island intensity (SUHII), and land-cover data were derived from these scenes. Results showed that Basra recorded the highest maximum LST in winter, spring, and autumn, whereas Mosul reached the highest summer peak (60.9 ℃). Baghdad exhibited the widest spatial extent of elevated summer temperatures, with the 50.1–59.8 ℃ class covering approximately 62.3% of its area. Basra recorded the highest SUHII in winter (7.8 ℃), Baghdad in spring (10.8 ℃), and Mosul in summer (12.9 ℃) and autumn (8.5 ℃). These findings revealed distinct urban thermal patterns: Mosul exhibits a pronounced summer peak, Baghdad shows a broader distribution of elevated temperatures, and Basra shows greater seasonal persistence. The results also revealed spatial and temporal variations in surface temperatures between Mosul, Baghdad, and Basra, linked to differences in land cover characteristics, the distribution of built-up areas, barren land, vegetation cover, and water bodies. Spatial comparisons further revealed variations in thermal patterns depending on surface characteristics and the geographical location of each city, reflecting the multiple factors involved in the formation of surface heat islands. The findings indicated a spatial correlation between the distribution of certain land cover types and thermal variations, without implying a direct causal relationship between human activities and rising surface temperatures.

1. INTRODUCTION

Urban heat islands are among the most prominent climatic consequences of urbanization. Converting natural surfaces into impermeable ones alters the surface energy balance, increasing heat storage and decreasing evaporation, resulting in temperature differences between urban and surrounding rural areas. The development of Remote Sensing (RS) technologies and Geographic Information Systems (GIS) has contributed to the spatial analysis of this phenomenon, relying on land surface temperature (LST) and surface urban heat island intensity (SUHII), which is calculated from the temperature difference between urban and rural areas [1-5]. Previous studies indicate that thermal patterns vary between cities and seasons depending on geographical location, climatic conditions, and land cover characteristics. A study of six cities in South Korea demonstrated variations in heat island intensity based on coastal and inland locations and climatic factors, confirming that population size alone does not explain thermal variations [6]. A study in Singapore also showed a correlation between thermal variation and land use, human activities, vegetation cover, and weather conditions [7]. These factors are particularly important in hot, arid, and semi-arid environments, where open land, water bodies, and vegetation cover influence the regulation of local temperatures [8-11]. In Iraq, the study of urban heat islands is gaining increasing importance due to urban expansion, the intensity of thermal conditions, and the variation in land cover characteristics among cities. A study in Baghdad revealed an inverse relationship between the intensity of heat islands and green spaces, as opposed to a direct relationship with building and road density [12]. Although previous Iraqi studies have addressed the phenomenon by analyzing temporal variations or comparing cities and examining its relationship to land cover, there remains a need for a comparative assessment that integrates seasonal variation, spatial extent, and heat island intensity within a unified analytical framework, especially in cities with diverse climatic and urban characteristics. Accordingly, this study aims to assess urban surface heat islands in the cities of Mosul, Baghdad, and Basra during 2025, using Landsat satellite data. It analyzes the four seasons using the LST and SUHII indices, and correlates their spatial distribution with land cover characteristics. The study's scientific contribution lies in comparing the three cities in

terms of peak temperature timing, heat island intensity, and the spatial extent of high-temperature categories. This comparison reveals their differing seasonal responses and clarifies the role of land cover characteristics and local environmental conditions in explaining the thermal variations between them. The study defined the urban area as the built-up areas within the boundaries of each city for the year 2025, while the rural area was represented by the area surrounding the outer boundaries of the urban area, with a uniform extension of 6 km. Water bodies, built-up areas, and all types of non-rural land uses were excluded from the rural area, in order to reduce the effect of heterogeneous surfaces in determining the reference temperature for each season during that year.

2. MATERIALS AND METHODS

2.1 Study area

The city of Mosul is located astronomically between latitudes 36°17′23″–36°25′45″ N and longitudes 43°02′59″–43°17′57″ E. Geographically, it is situated in the northwestern part of Iraq. Baghdad, on the other hand, is located astronomically between latitudes 33°11′00″-33°29′00″ N and longitudes 44°11′00″–44°34′00″ E, occupying a central and strategic location. Basra is geographically located in southern Iraq, at approximately 30°30′00″ N latitude and 47°48′00″ E longitude. The urban study area covers approximately 155 km² (Figure 1).

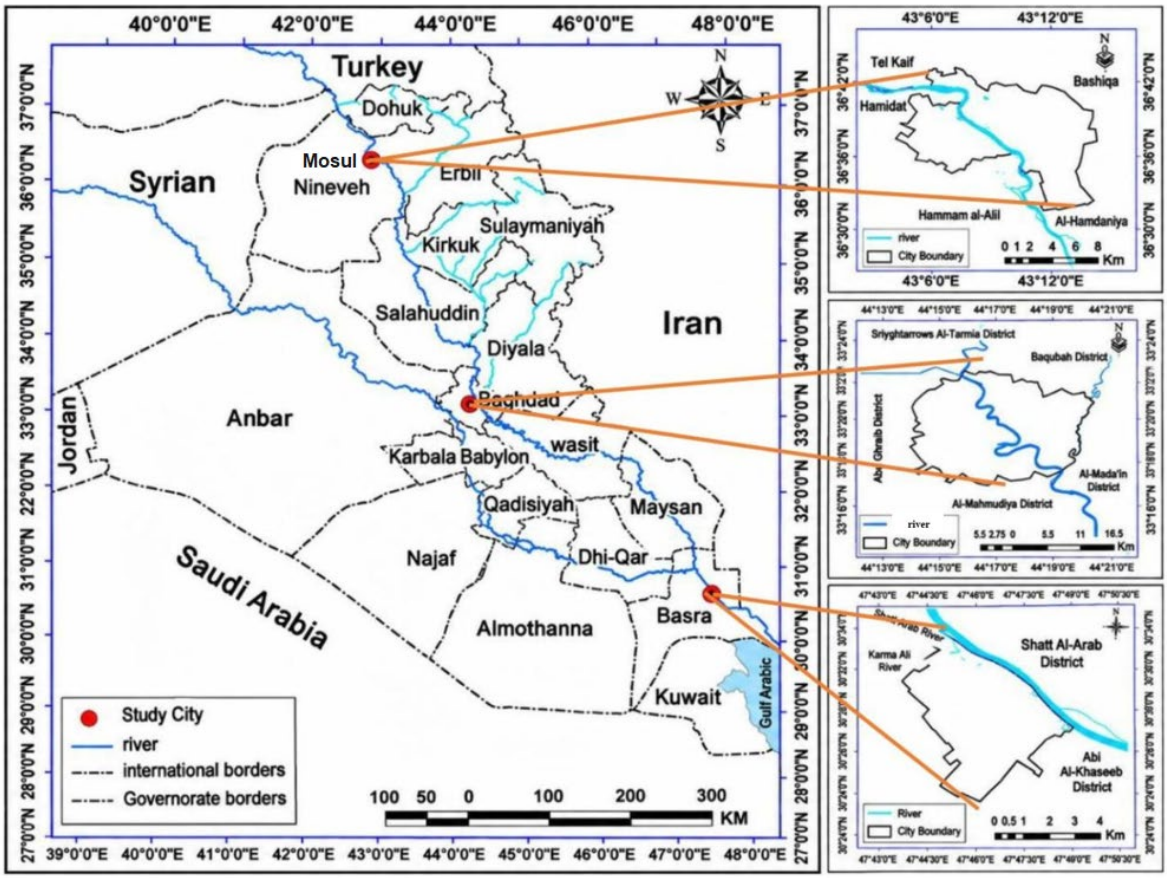

Figure 1. The study area

2.2 Data

This study relied on satellite imagery acquired by the Landsat 9 satellite, equipped with the Operational Land Imager-2 (OLI-2) and the Thermal Infrared Sensor-2 (TIRS-2), for the year 2025. These images were selected because they provide spectral and thermal data suitable for retrieving LST, as well as for examining the spatial variations of surface urban heat islands (SUHIs). A total of 12 Landsat 9 satellite scenes were selected, comprising four scenes for each study city (Mosul, Baghdad, and Basra), with one scene representing each of the four seasons (winter, spring, summer, and autumn) during 2025. The satellite scenes were acquired on different dates across the three study cities during the four seasons of 2025, as detailed in Table 1, to capture seasonal variations in LST. The selection of satellite imagery for the four seasons was based on scene availability, image clarity, and minimal cloud cover, as far as possible, to ensure the consistency and reliability of comparisons among the study cities of Mosul, Baghdad, and Basra, as presented in Table 1.

The study also employed Landsat Collection 2 Level-2 products, which undergo processing and corrections that make them suitable for subsequent analysis. Thermal data were used to retrieve LST, while spectral data were utilized to calculate the Normalized Difference Vegetation Index (NDVI), the Normalized Difference Built-up Index (NDBI), and the Normalized Difference Water Index (NDWI). These indices were employed to investigate the influence of vegetation cover, built-up areas, and water resources on the spatial variability of LST.

The satellite imagery was obtained from the official website of the United States Geological Survey (USGS). The data were subsequently processed within a GIS environment and prepared in accordance with the spatial boundaries of the study

cities.

2.3 Methodology

This study adopted a comparative analytical approach integrating GIS and RS to assess the spatial and seasonal characteristics of SUHIs in the study cities during 2025. The workflow began with satellite image preparation and the retrieval of LST, followed by interpretation in relation to land cover and spectral indices. The thermal difference between the urban area and a reference rural buffer was then determined, followed by statistical and spatial comparisons among the study cities.

Table 1. Characteristics of the satellite imagery used in the study for the year 2025

City	Season	Path/Row	Product ID	Acquisition Date	Acquisition Time (UTC)	Cloud Cover (%)	Valid Pixels (%)
Mosul	Winter	035/170	LC09_L2SP_170035_20250115_20250117_02_T1	2025/1/15	07:38:12 UTC	1.15%	98.85%
Mosul	Spring	035/170	LC09_L2SP_170035_20250420_20250422_02_T1	2025/4/20	07:38:05 UTC	0.42%	99.58%
Mosul	Summer	035/170	LC09_L2SP_170035_20250725_20250727_02_T1	2025/7/25	07:38:22 UTC	0.00%	100.00%
Mosul	Autumn	035/170	LC09_L2SP_170035_20251029_20251031_02_T1	2025/10/29	07:38:18 UTC	0.08%	99.92%
Baghdad	Winter	037/168	LC09_L2SP_168037_20250131_20250202_02_T1	2025/1/31	07:25:44 UTC	2.05%	97.95%
Baghdad	Spring	037/168	LC09_L2SP_168037_20250506_20250508_02_T1	2025/5/6	07:25:38 UTC	0.18%	99.82%
Baghdad	Summer	037/168	LC09_L2SP_168037_20250810_20250812_02_T1	2025/8/10	07:25:50 UTC	0.00%	100.00%
Baghdad	Autumn	037/168	LC09_L2SP_168037_20251114_20251116_02_T1	2025/11/14	07:25:41 UTC	0.00%	100.00%
Basra	Winter	039/166	LC09_L2SP_166039_20250216_20250218_02_T1	2025/2/16	07:13:10 UTC	3.12%	96.88%
Basra	Spring	039/166	LC09_L2SP_166039_20250522_20250524_02_T1	2025/5/22	07:13:02 UTC	0.05%	99.95%
Basra	Summer	039/166	LC09_L2SP_166039_20250826_20250828_02_T1	2025/8/26	07:13:16 UTC	0.00%	100.00%
Basra	Autumn	039/166	LC09_L2SP_166039_20251130_20251202_02_T1	2025/11/30	07:13:08 UTC	0.10%	99.90%

2.3.1 Satellite image preparation and atmospheric correction

The study employed Landsat 9 imagery from the Collection 2 Level-2 products, which provide surface reflectance and surface temperature data suitable for quantitative analysis. Image processing was conducted using a unified coordinate reference system, and the images were clipped to the boundaries of the study cities.

In addition, the Quality Assessment Pixel (QA_PIXEL) band was examined to exclude pixels affected by cloud cover and cloud shadows before analysis.

Atmospheric correction of the spectral bands was not performed manually because the Level-2 Surface Reflectance product had already undergone atmospheric correction using the Land Surface Reflectance Code (LaSRC) algorithm. This algorithm converts top-of-atmosphere reflectance into surface reflectance suitable for spectral analysis.

The official scaling factor provided by the USGS was applied to convert the digital numbers (DN) of the Landsat Collection 2 Level-2 spectral bands into surface reflectance, according to the following equation:

$$SR = (DN \times 0.0000275) - 0.2$$

where,

SR = Surface reflectance.

DN = Pixel digital number.

The spatial resolution of the optical bands is 30 m, whereas the native spatial resolution of the thermal bands is 100 m. The thermal data are distributed within Landsat products after resampling to a 30 m grid.

2.3.2 Land surface temperature retrieval

Thermal analysis was based on the Surface Temperature product included in Landsat Collection 2 Level-2, particularly the ST_B10 band derived from the TIRS-2 Band 10. Unlike sensor brightness temperature, the Level-2 LST product is generated using established thermal retrieval algorithms that incorporate surface emissivity and auxiliary atmospheric inputs. The following equation was used to convert the DN of the ST_B10 band into Kelvin:

$$ST\ (K) = (DN \times 0.00341802) + 149.0$$

The resulting temperatures were then converted from Kelvin to degrees Celsius using the following equation:

$$LST\ (°C) = ST\ (K) - 273.15$$

Using these transformations, the mean and maximum LSTs were calculated for each study city and each season. The LST maps were also reclassified into several temperature classes to quantify the spatial extent of hotter areas and facilitate comparisons among the study cities.

2.3.3 Land cover and spectral indices

A unified land-cover classification scheme was adopted to facilitate spatial comparisons among the study cities. The classification comprised four principal categories: built-up areas, vegetation cover, water bodies, and barren or vacant lands. The resulting land-cover maps were used to interpret the spatial distribution of LST.

Land-cover maps were produced using supervised classification of Landsat 9 imagery at a spatial resolution of 30 m, based on the 12 seasonal satellite scenes listed in Table 1. The NDVI, NDBI, and NDWI indices were also used to interpret land-cover characteristics. Three supplementary spectral indices were calculated from the atmospherically corrected spectral bands: the NDVI, the NDBI, and the NDWI. The Landsat 9 bands used were Band 3 (green), Band 4 (red), Band 5 (near-infrared), and Band 6 (shortwave infrared). The indices were calculated using the following equations:

Normalized Difference Vegetation Index (NDVI):

$$NDVI = \frac{B5 - B4}{B5 + B4}$$

Normalized Difference Built-up Index (NDBI):

$$NDBI = \frac{B6 - B5}{B6 + B5}$$

Normalized Difference Water Index (NDWI):

$$NDWI = \frac{B3 - B5}{B3 + B5}$$

These indices helped interpret the thermal changes in relation to vegetation cover, built-up surfaces, and water resources in the study cities.

2.3.4 Urban area, rural buffer, and surface urban heat island intensity

The urban area was defined as the built-up area within each city's boundary. To define the rural reference zone, a uniform 6 km buffer was established beyond the urban fringe of each study city. Water bodies, built-up areas, and other land uses considered unrepresentative of the rural reference environment were excluded to limit the influence of thermally heterogeneous surfaces on the reference temperature. The mean LST was then computed for the urban area and the rural reference buffer of each study city.

The SUHII was calculated as the difference between mean urban and rural LST, using the following equation:

$$SUHII = LST_{Urban} - LST_{Rural}$$

where,

SUHII = Surface Urban Heat Island Intensity.

LST_{Urban} = Mean land surface temperature of the urban area.

LST_{Rural} = Mean land surface temperature of the rural reference buffer.

Accordingly, SUHII differs conceptually from the maximum LST. Thus, a city may record the highest absolute surface temperature without having the highest SUHII, for example, when the surrounding rural area is also relatively hot. This distinction is crucial for understanding the differences in urban thermal conditions among Mosul, Baghdad and Basra.

3. RESULTS

3.1 Thermal peaks and surface urban heat island intensity

As can be seen in the maximum LST values in Table 2, the rank of the study cities is different for each season. During winter, spring, and autumn, the maximum temperatures generally rise towards the south, with the highest recorded at Basra: 27.3 ℃ in winter, 53.2 ℃ in spring, and 50.3 ℃ in autumn. But the situation is remarkably different during summer, when the highest value (60.9 ℃) is recorded in Mosul, followed by Baghdad (59.8 ℃) and Basra (57.6 ℃). This study shows that thermal peaks cannot be explained only by climatic background; the local surface characteristics can be important in changing the relative thermal ranking of the cities in the hottest season [13].

Table 2. Seasonal maximum land surface temperature (LST) values in the study cities

Season	Mosul (℃)	Baghdad (℃)	Basra (℃)
Winter	20.2	24.1	27.3
Spring	47.8	48.9	53.2
Summer	60.9	59.8	57.6
Autumn	46.8	48.9	50.3

Table 3. Seasonal surface urban heat island intensity (SUHII) in the study cities during 2025

Season	Mosul (℃)	Baghdad (℃)	Basra (℃)	City with Highest Intensity
Winter	0.4	1.7	7.8	Basra
Spring	9.7	10.8	5.7	Baghdad
Summer	12.9	7.4	4.5	Mosul
Autumn	8.5	4.5	4.4	Mosul

Regarding SUHII, Table 3 shows that the highest intensity occurred in Basra in winter (7.8 ℃), in Baghdad in spring (10.8 ℃), and in Mosul in summer and autumn (12.9 ℃ and 8.5 ℃, respectively). These results show that SUHII does not depend solely on the maximum LST recorded at a specific site, but rather on the difference between urban and rural temperatures. Thus, the city with the highest thermal peak does not necessarily exhibit the strongest SUHI effect.

Table 4. Average city and surrounding countryside temperatures by season for the study area

Season	Mosul (℃)		Baghdad (℃)		Basra (℃)	
	City	Countryside	City	Countryside	City	Countryside
Winter	12.2	11.8	18.3	16.6	23.6	15.8
Spring	42.1	32.4	43.7	32.9	47.1	41.4
Summer	54.7	41.8	53.1	45.7	53.3	48.8
Autumn	39.4	30.9	40.9	36.4	43.3	38.9

The data in Table 4 reveal a variation in average surface temperature between urban and rural areas in the studied cities throughout the year, with urban areas recording higher temperatures than rural areas in all cases studied. These averages were used to calculate the SUHII by finding the difference between the average surface temperature in the urban area and the average in the rural area for each city and season. The calculated values are consistent with the results

presented in Table 3, confirming the consistency of the data and the calculation results.

3.2 Spatial extent of high-temperature areas

Because of the contrast between the thermal peaks and the spatial range of elevated temperature, the summer data given in Table 5 show this. In Mosul, the upper temperature class (>50 ℃) is approximately 48.2% of the area of the city, while in Baghdad it is 62.3% and in Basra it is 60.0%. Hence, although Mosul has the highest maximum LST, Baghdad has the largest spatial dominance of the upper temperature class. The difference shows that Baghdad is more likely to be described as a city with a more widely spread spatial distribution of high summer temperatures than the other two study cities.

Table 5. Relative spatial extent of high-temperature areas during summer 2025

City	Area within 40.1–50.0 ℃ (%)	Area within the Upper Temperature Class (>50 ℃) (%)	Total Area above 40 ℃ (%)
Mosul	49.1	48.2	97.3
Baghdad	36.2	62.3	98.5
Basra	36.1	60.0	96.1

3.3 Seasonal persistence of high-temperature areas

Seasonal persistence can be seen in the percentage of LST values that are greater than or equal to 40.1 ℃ for each city. The spatial percentages give a much better indication of thermal conditions than isolated maximum temperature values, as shown in Table 5.

In spring, the percentage of area with temperature equal to or greater than 40.1 ℃ is 19.7% in Mosul, 52.5% in Baghdad, and 93.0% in Basra (Table 6). This pattern indicates that elevated surface temperatures become spatially widespread in Basra earlier in the annual cycle than in the other study cities. During the summer thermal peak, high-temperature conditions become nearly ubiquitous across all three cities, covering 97.3% of Mosul, 98.5% of Baghdad, and 96.1% of Basra. However, the differences become more pronounced during autumn, when the proportion declines to 13.2% in Mosul and 30.1% in Baghdad, while remaining substantially higher in Basra at 72.0%.

These findings indicate that Basra's distinctive thermal characteristic is not its maximum summer temperature, but rather the longer seasonal persistence and broader temporal distribution of high-temperature conditions before and after summer. Baghdad is characterized by the most extensive summer coverage of areas exceeding 40 ℃, whereas Mosul exhibits a pronounced summer thermal peak followed by a rapid autumnal contraction of the high-temperature zone.

3.4 Spatial interpretation in relation to land cover

LST is not distributed uniformly within urban environments. Instead, its spatial pattern is influenced by surface characteristics, vegetation cover, building density, water resources, and vacant or barren lands. Accordingly, the spatial distribution of temperature represents a key dimension of urban heat island analysis, helping explain the causes of intra-urban thermal variability [4]. On this basis, the study compares four common land-cover classes across the three cities: vegetation cover, water bodies, built-up areas, and vacant or barren lands, as presented in Table 7. This comparison provides a framework for examining how differences in land-cover composition contribute to the observed spatial variations in LST among Mosul, Baghdad, and Basra.

Table 6. Seasonal variation in the proportion of land area with land surface temperature (LST) >40 ℃ in the study cities during 2025

City	Winter (%)	Spring (%)	Summer (%)	Autumn (%)	Principal Annual Thermal Characteristic
Mosul	0.0	19.7	97.3	13.2	Pronounced summer peak followed by rapid autumnal contraction
Baghdad	0.0	52.5	98.5	30.1	Nearly citywide summer expansion of high-temperature areas
Basra	0.0	93.0	96.1	72.0	Early onset and prolonged persistence of high-temperature conditions

Table 7. Relative composition of land cover in the study cities

City	Vegetation Cover (%)	Water Cover (%)	Built-Up Areas (%)	Vacant/Barren Land (%)
Mosul	16.7	3.1	39.5	40.7
Baghdad	9.6	2.3	62.2	25.9
Basra	9.0	4.5	69.1	17.4

3.4.1 Mosul

Mosul exhibits a relatively balanced spatial structure, with built-up areas accounting for 39.5% of its total area and vacant and dry lands covering approximately 40.7%. Vegetation cover is also substantial, accounting for 16.7%, the highest proportion among the study cities, while water bodies represent 3.1% of the city's area. Overlaying the city's land cover map on its LST maps showed that hot spots do not correspond only to the distribution of built-up areas. The widespread bare and exposed surfaces absorb large amounts of solar radiation and heat up rapidly, while the vegetated patches and the river corridor act as zones of relative cooling, interrupting the spatial continuity of high-temperature surfaces. This partly explains why the summer surface temperature in Mosul is high, although its built-up proportion is smaller than those of Baghdad and Basra. This strong thermal response to solar radiation is attributed to limited surface moisture and the predominance of dry surface materials over large areas [14].

3.4.2 Baghdad

Baghdad is clearly dominated by built-up areas (62.2% of

study area) and vacant and barren lands (25.9%). Only 9.6% of the area is vegetated, and 2.3% is water bodies. The high spatial density of impervious and dry surfaces created by this land-cover composition is reflected in the wide spatial coverage of the upper temperature classes in the LST maps. Meanwhile, the continuous and discontinuous green spaces, in combination with the Tigris River, create relatively cooler corridors and thermal refuges in the city. Their cooling effect is, however, limited in space as compared to the enormous built-up bulk [15].

3.4.3 Basra

Basra has the highest percentage of built-up area, about 69.1% of the study area. The areas of vacant and bare lands are 17.4%, the vegetation cover is about 9.0%, and water bodies are about 4.5%. The composition corresponds to a very urbanized surface structure, the relatively high surface cover of waters a special spatial structure. If these water bodies and waterways can create localized cooling zones, the surrounding built-up and dry surfaces tend to heat up more under the solar radiation. The relationship shown in the LST maps is that a higher percentage of built-up land is not necessarily correlated with the highest absolute LST. Atmospheric conditions, surface moisture, and surface materials' thermal properties also affect peak surface heating. On the other hand, the percentage of built-up land can be used to assess the spatial coverage of the urban surface environment where heat can be stored. The spatial thermal pattern of Basra can thus be described as a mosaic of hot urban spaces and relatively cold water corridors with small and restricted vegetation cover that can be utilized to prolong the cooling effect.

3.5 Seasonal and spatial interpretation

The difference in the LST between seasons is not only represented by seasonal variations in temperature. They also show the spatial variation of thermal conditions within a city due to the influence of solar energy, climatic seasons, and surface characteristics. Accordingly, this study examines thermal variability from three aspects: (1) the occurrence of thermal peaks; (2) the continuity of high-temperature areas from one season to the next; and (3) the spatial extent of the different temperature classes. A high peak temp could be accompanied by a small spatial extent of high temperatures, while another city could experience a lower peak temp, and a much larger spatial extent of high temperatures. The latest research focuses on the integration of spatial mapping along with seasonal analysis and surface characteristics in the interpretation of urban heat islands [12]. To enhance the spatial analysis, the LST map of each study city was combined with its urban land use map in a single panel for each season. This facilitates comparison of the location of thermal classes with urban surface patterns, such as vegetation cover, water bodies, built-up areas, vacant land, and industrial/commercial areas.

3.5.1 Winter

There is significant thermal variation among the different study cities, as seen from the maps (Figures 2–4) and the winter data in Table 8. These differences are not only with regard to the highest temperature class but also the percentage of the city's area covered by each temperature class. In Mosul, the class 10.1–20 ℃ covers approximately 75.9% of the area, whereas the class above 20 ℃ covers only 0.4%. This distribution indicates that hot spots of relatively warm temperatures are also spatially constrained in the cold season. Baghdad's thermal pattern is more homogeneous, with the 10.1–20 ℃ class covering 96.7% of the area of the city. Winter temperatures are very concentrated in the intermediate range, with only 3.2% of the area in the higher class (20.1–24.1 ℃).

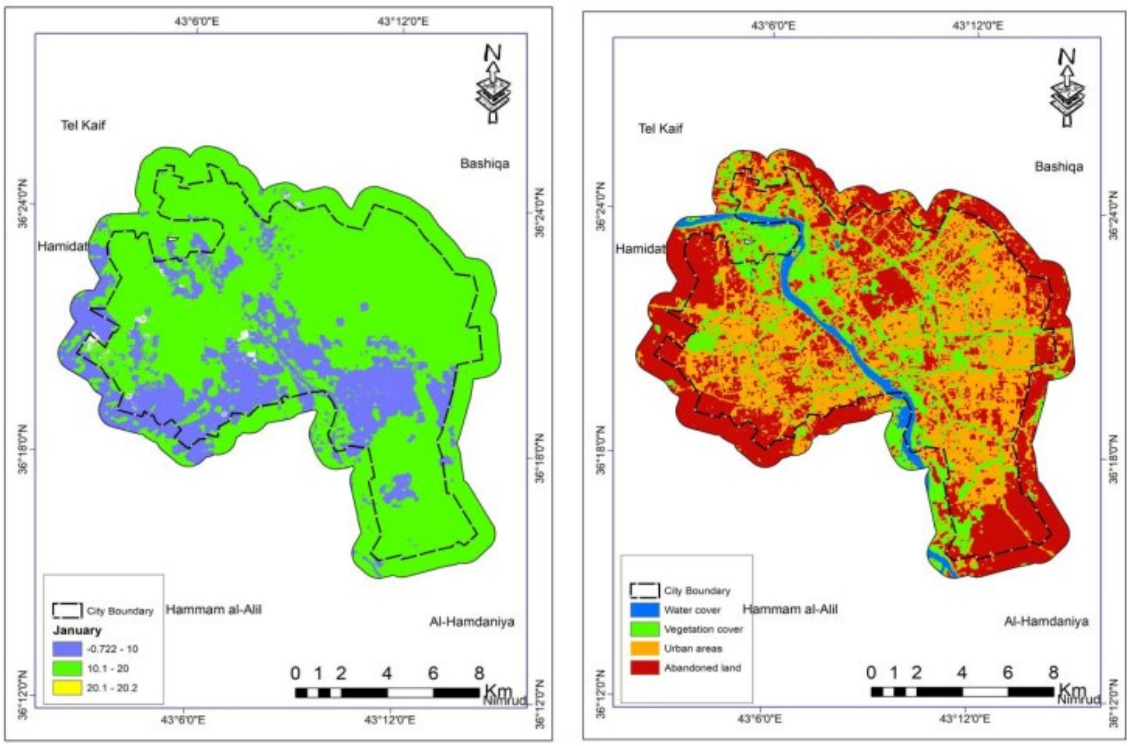

Figure 2. Spatial comparison between ground surface temperature and urban land uses in the city of Mosul during the winter of 2025

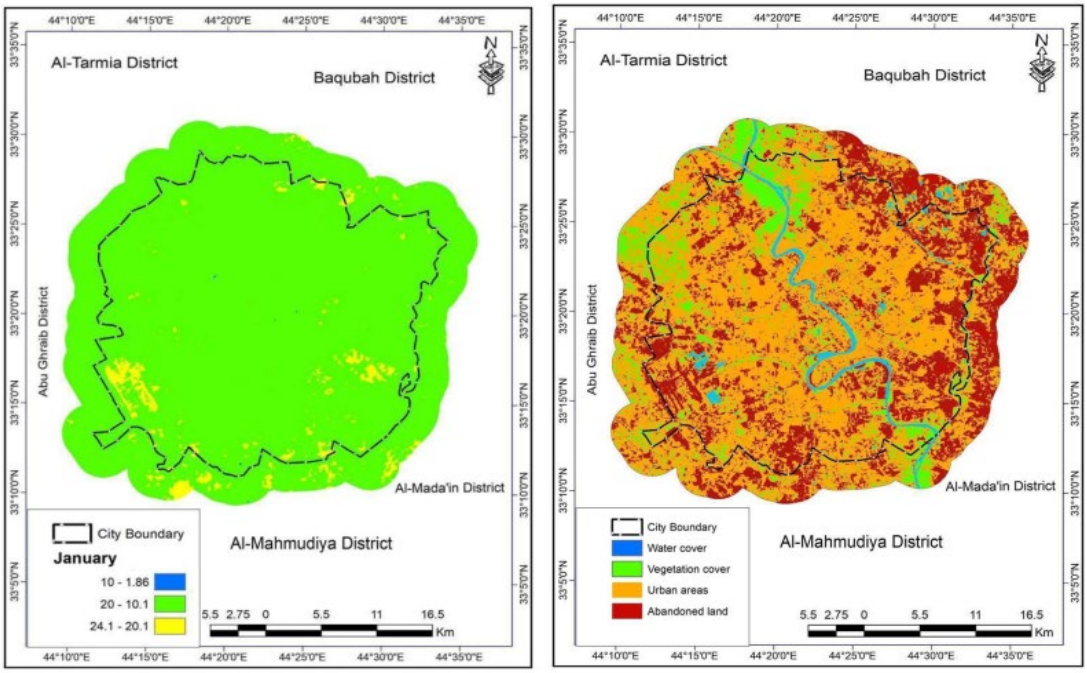

Figure 3. Spatial comparison between ground surface temperature and urban land uses in Baghdad during the winter of 2025

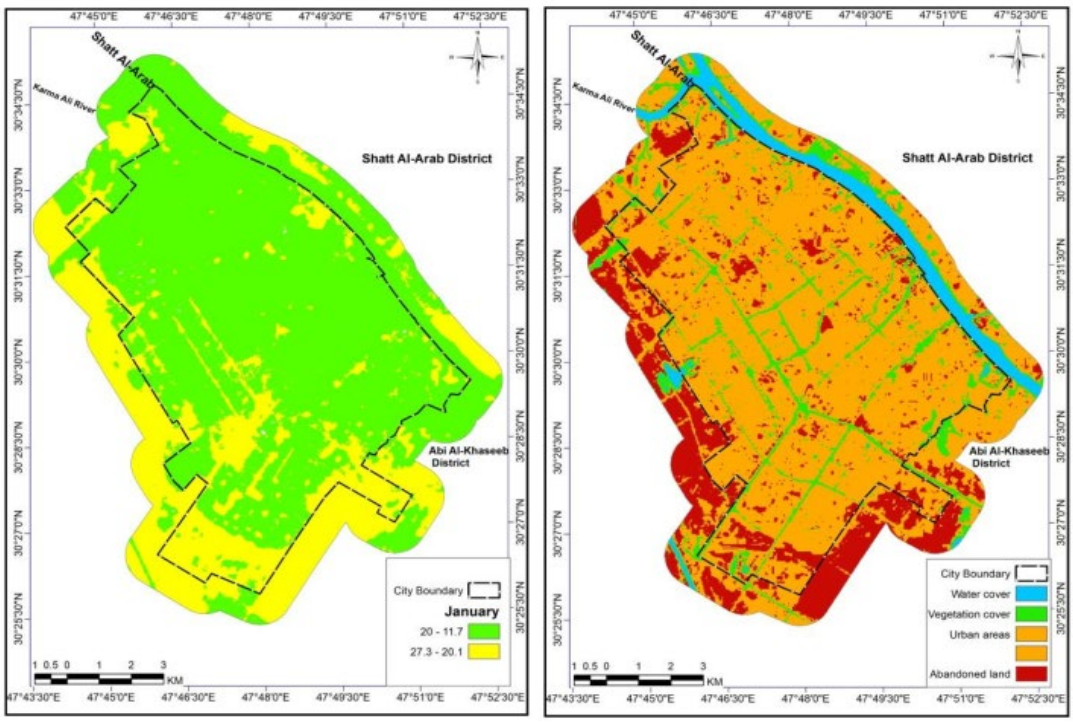

Figure 4. Spatial comparison between ground surface temperature and urban land uses in the city of Basra during the winter of 2025

Table 8. Distribution, area, and percentage of land surface temperature (LST) classes in the study cities during the winter of 2025

City	Temperature Class (°C)	Area (km²)	Percentage (%)
Mosul	≤10	54	23.7
Mosul	10.1–20.0	173	75.9
Mosul	20.1–20.2	1	0.4
Baghdad	≤10	1	0.1
Baghdad	10.1–20.0	1,239	96.7
Baghdad	20.1–24.1	41	3.2
Basra	11.7–20.0	105	67.7
Basra	20.1–27.3	50	32.3

Basra has a more distinct spatial gradient in the transition to a higher temperature range of the three cities. The 20.1–27 ℃ class covers about 32.3% of the study area. So the predominance of the winter thermal class in Basra is not only due to the maximum recorded temperature but also to the larger area of the relatively warm surfaces.

This result validates the use of LST as a spatial parameter (not a single value) and interpretation based on the spatial variation of land cover classes and their thermal properties. Overall, the winter season represents the annual thermal cycle baseline for each city, as Mosul exhibits a lower temperature and higher variability, Baghdad exhibits relatively warm

temperatures and higher homogeneity in the intermediate temperature class, and Basra exhibits a broader distribution of warmer temperature classes. The seasonal baseline is an important reference point for determining how quickly each city warms up in the spring and summer, and how well it can maintain warm conditions as it cools down in the fall.

3.5.2 Spring

An examination of Figures 5–7 and the data presented in Table 9 indicates that spring represents the most revealing transitional phase, owing to differences in the pace of surface heating among the study cities [16].

In Mosul, the 30.1–40.0 ℃ temperature class dominates, accounting for 77.6% of the city's area, whereas areas exceeding 40 ℃ represent only 19.7%. This distribution indicates that, although surface temperatures increase substantially compared with winter, elevated temperatures have not yet developed into a spatially dominant feature across the city [14].

Baghdad, by contrast, enters a more advanced transitional phase during spring. The 40.1–48.9 ℃ temperature class accounts for 52.5% of the study area, compared with 46.3% for the 30.1–40.0 ℃ class. This means that over 50% of the study area has fallen into the class of high temperatures, where it is above 40 ℃. This is probably related to the wide built-up area of Baghdad city because some land-use changes and variation in vegetation density and urban activity are responsible for the spatial variation in LST.

Basra exhibits pronounced seasonal surface warming, with a maximum temperature of 53.2 ℃. Its distinctive thermal characteristic is the extensive distribution of the 40.1–50.0 ℃ class, covering 92.2% of the study area, whereas temperatures exceeding 50 ℃ account for only 0.8%. Overall, the spring shows a distinct gradient in timing the transition towards hot-season conditions. This transition has occurred relatively slowly in Mosul; it is more developed in Baghdad, and it occurred earlier and is more spatially extensive in Basra. These differences underscore the need to consider, in addition to the maximum temperatures, the spatial distribution of temperature classes when making comparisons of seasonally defined thermal dynamics in cities.

Table 9. Distribution, area, and percentage of land surface temperature (LST) classes in the study cities during the spring of 2025

City	Temperature Class (℃)	Area (km²)	Percentage (%)
Mosul	15.5–20.0	1	0.4
Mosul	20.1–30.0	5	2.3
Mosul	30.1–40.0	177	77.6
Mosul	40.1–47.8	45	19.7
Baghdad	23.8–30.0	15	1.2
Baghdad	30.1–40.0	594	46.3
Baghdad	40.1–48.9	673	52.5
Basra	26.6–30.0	4	2.3
Basra	30.1–40.0	7	4.7
Basra	40.1–50.0	143	92.2
Basra	50.1–53.2	1	0.8

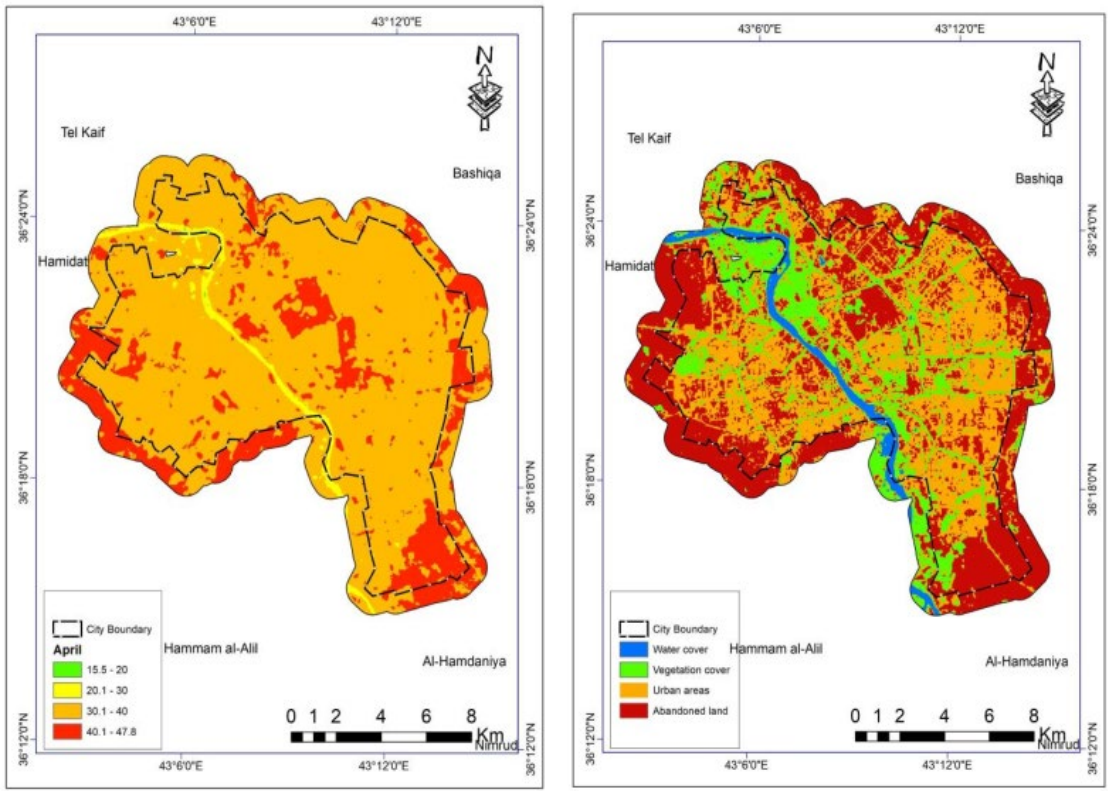

Figure 5. Spatial comparison between ground surface temperature and urban land uses in the city of Mosul during the spring of 2025

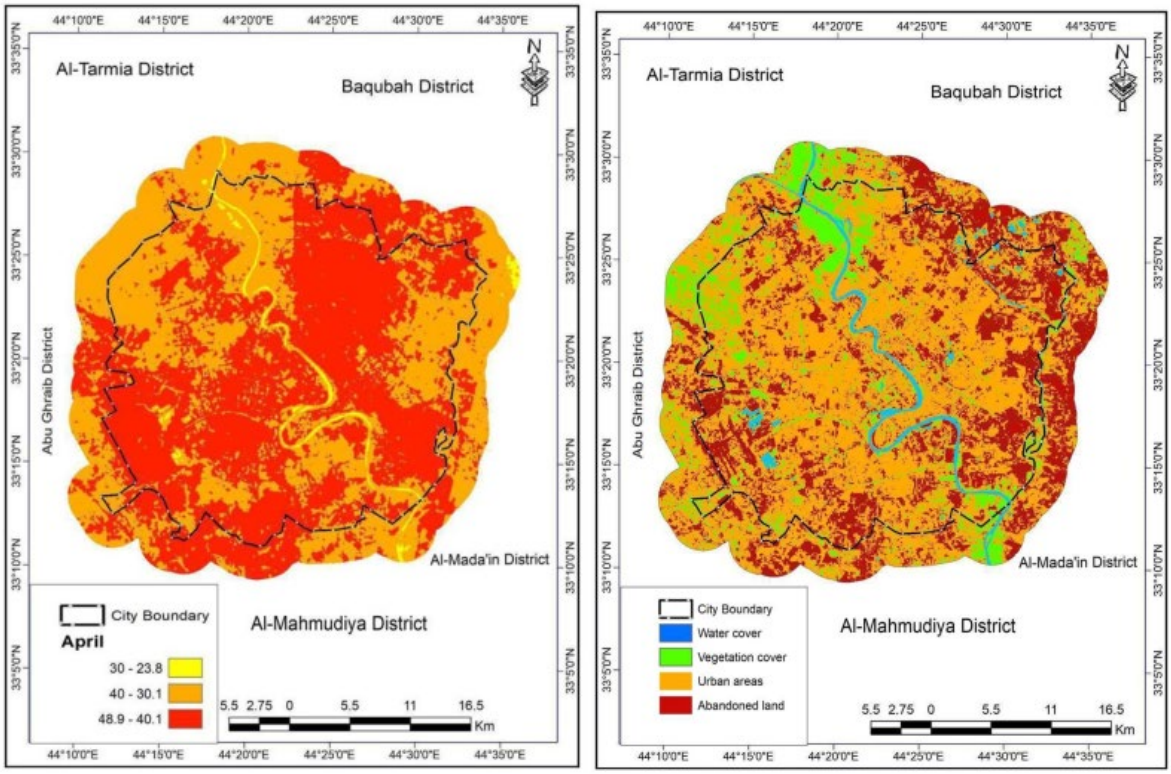

Figure 6. Spatial comparison between ground surface temperature and urban land uses in the city of Baghdad during the spring of 2025

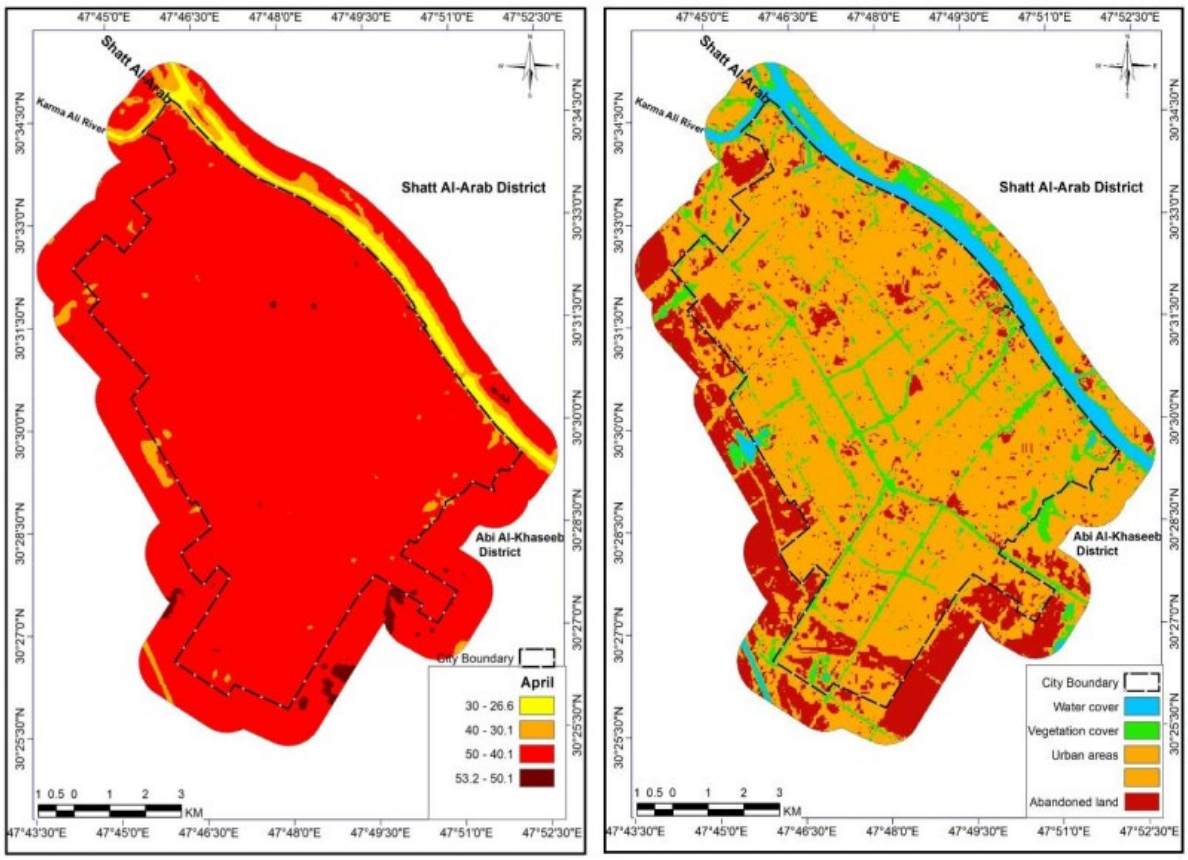

Figure 7. Spatial comparison between ground surface temperature and urban land uses in the city of Basra during the spring of 2025

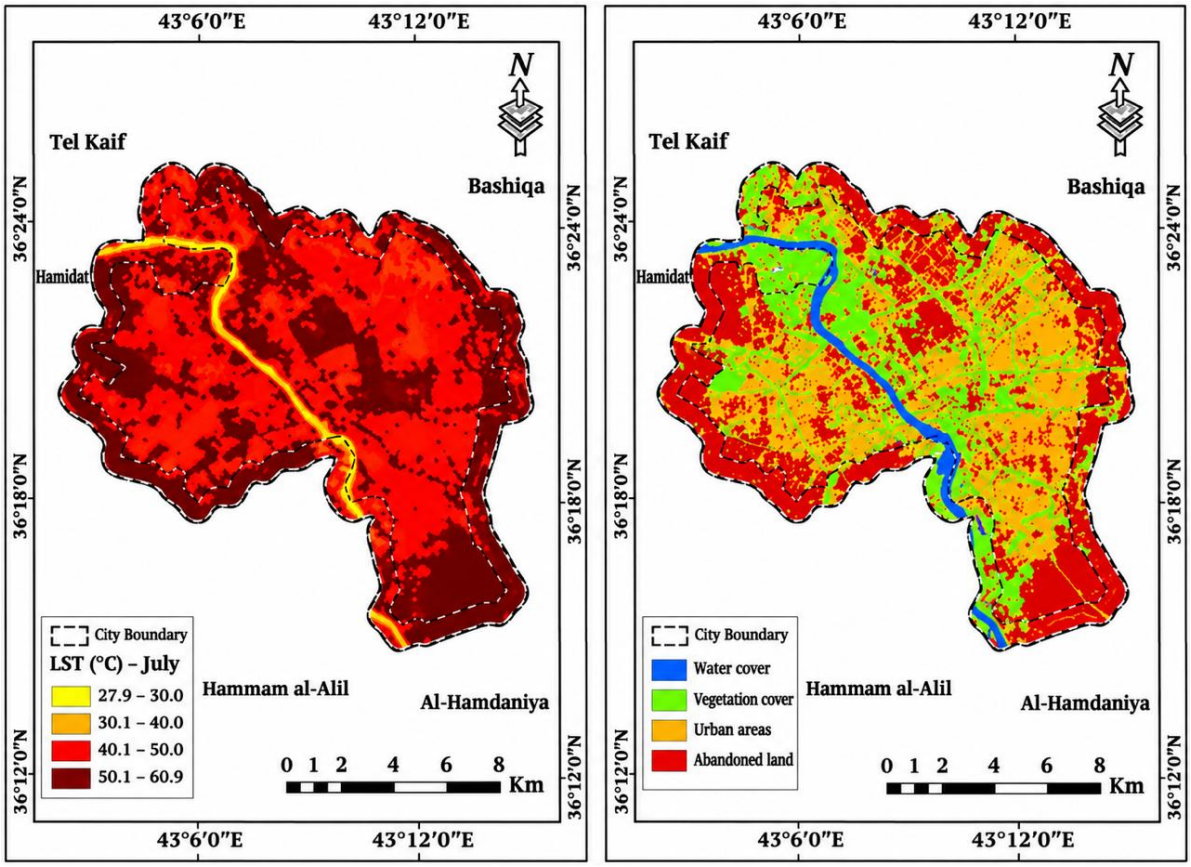

Figure 8. Spatial comparison between ground surface temperature and urban land uses in the city of Mosul during the summer of 2025

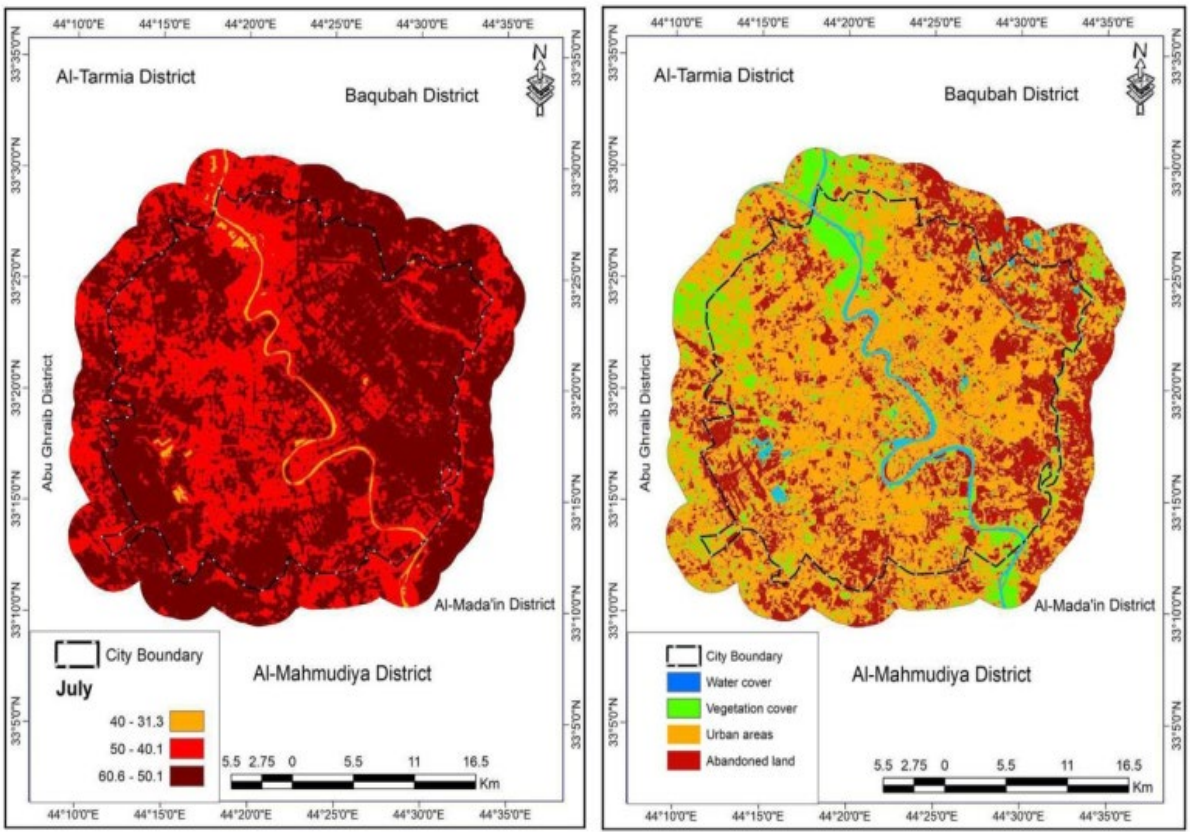

Figure 9. Spatial comparison between ground surface temperature and urban land uses in Baghdad during the summer of 2025

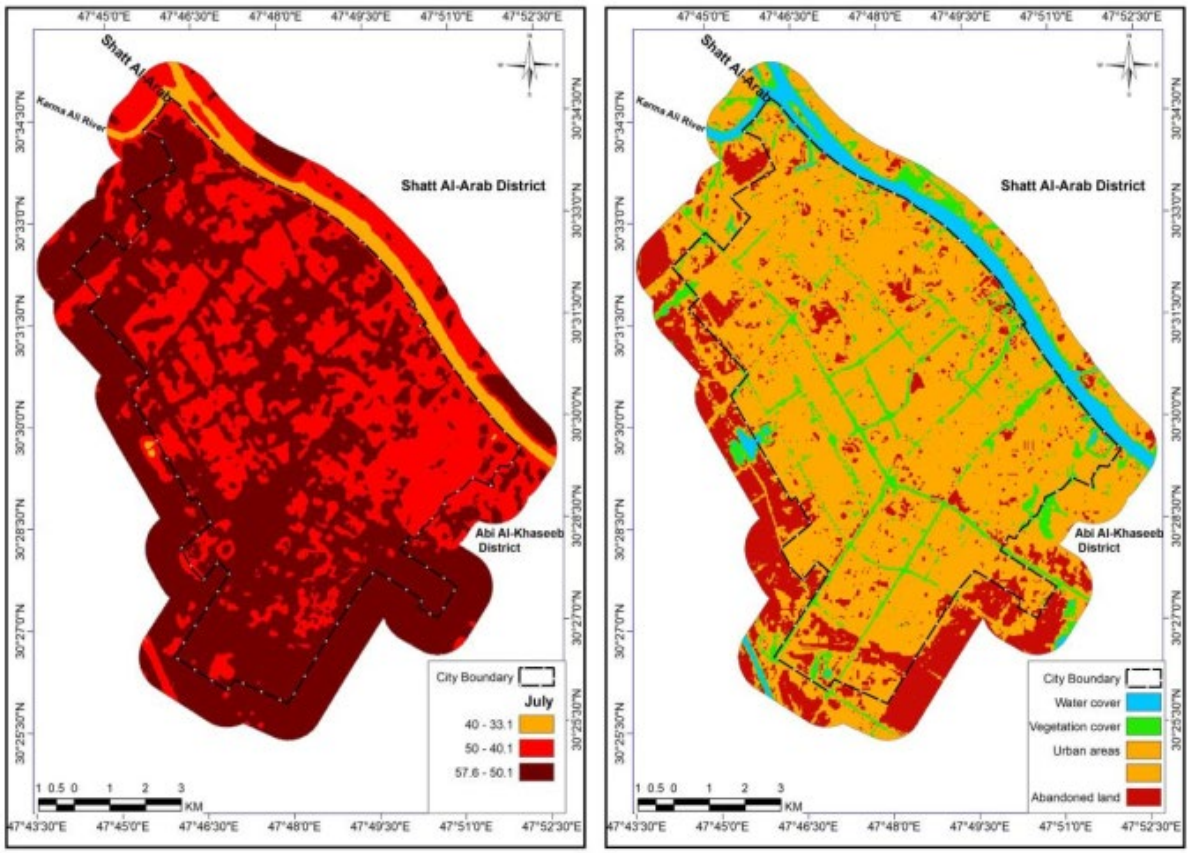

Figure 10. Spatial comparison between ground surface temperature and urban land uses in the city of Basra during the summer of 2025

3.5.3 Summer

Examination of Figures 8–10 and the data in Table 10 shows that summer represents the peak of the annual thermal cycle in all three study cities in 2025. However, a clear distinction emerges between the maximum intensity of the thermal signal and the spatial extent of the warm areas [17].

Mosul records the highest maximum LST (60.9 ℃). However, the 50.1–60.9 ℃ class covers 48.2% of the city's area, while the 40.1–50.0 ℃ class accounts for 49.1%. The close proportions of these two classes show that Mosul's extremely high thermal peak does not mean that the highest temperature range is spatially dominant there. Instead, it reflects the strong thermal response of specific surfaces within a more complex urban thermal structure. The highest LST in Baghdad (59.8 ℃) is slightly lower than that of Mosul. However, its 50.1–59.8 ℃ class is the most extensive among the study cities, covering 62.3% of the city area. Indeed, the most distinctive feature of Baghdad's summer thermal regime is the strong spatial predominance of the upper temperature class. This trend is similar to findings in highly urbanized regions, where intensive urban land use and reduced vegetation can raise surface temperatures. The highest LST recorded in Basra is 57.6 ℃, lower than that of Mosul and Baghdad. Nevertheless, the 50.1–57.6 ℃ class covers 60.0% of the study area, indicating the widespread presence of high surface temperatures. These results reveal three distinct summer thermal regimes: Mosul has the highest localized thermal peak, Baghdad has the most widespread spatial dominance of the upper temperature class, and Basra shows an extensive spatial distribution of intensely heated surfaces despite having the lowest maximum LST. The results confirm that surface thermal patterns are driven by the maximum temperature, but should also consider the spatial extent of the SUHI and land-cover characteristics to provide a more complete view of urban thermal variability [18].

Table 10. Distribution, area, and percentage of land surface temperature (LST) classes in the study cities during the summer of 2025

City	Temperature Class (℃)	Area (km²)	Percentage (%)
Mosul	27.9–30.0	1	0.5
Mosul	30.1–40.0	5	2.2
Mosul	40.1–50.0	112	49.1
Mosul	50.1–60.9	110	48.2
Baghdad	31.1–40.0	19	1.5
Baghdad	40.1–50.0	464	36.2
Baghdad	50.1–59.8	798	62.3
Basra	33.1–40.0	6	3.9
Basra	40.1–50.0	56	36.1
Basra	50.1–57.6	93	60.0

To further assess the summer LST extremes, a percentile-based analysis was conducted using the available LST raster data for Mosul and Baghdad in 2025. The 95th percentile (P95) values were 55.13 ℃ and 54.08 ℃, respectively, while the 99th percentile (P99) values reached 56.53 ℃ and 55.44 ℃. The maximum recorded LST values were 60.94 ℃ in Mosul and 59.77 ℃ in Baghdad. These findings indicate that Mosul exhibited higher upper-tail surface temperatures than Baghdad. However, the maximum values exceeded the corresponding P99 thresholds, highlighting the importance of examining extreme-temperature pixels and their quality before drawing definitive conclusions about the spatial reliability of these thermal peaks.

3.5.4 Autumn

An examination of Figures 11–13 and the data presented in Table 11 indicates that autumn is of particular analytical significance because it reveals not only the magnitude of the temperature decline relative to summer, but also the rate at which each city transitions out of the period of intense heat.

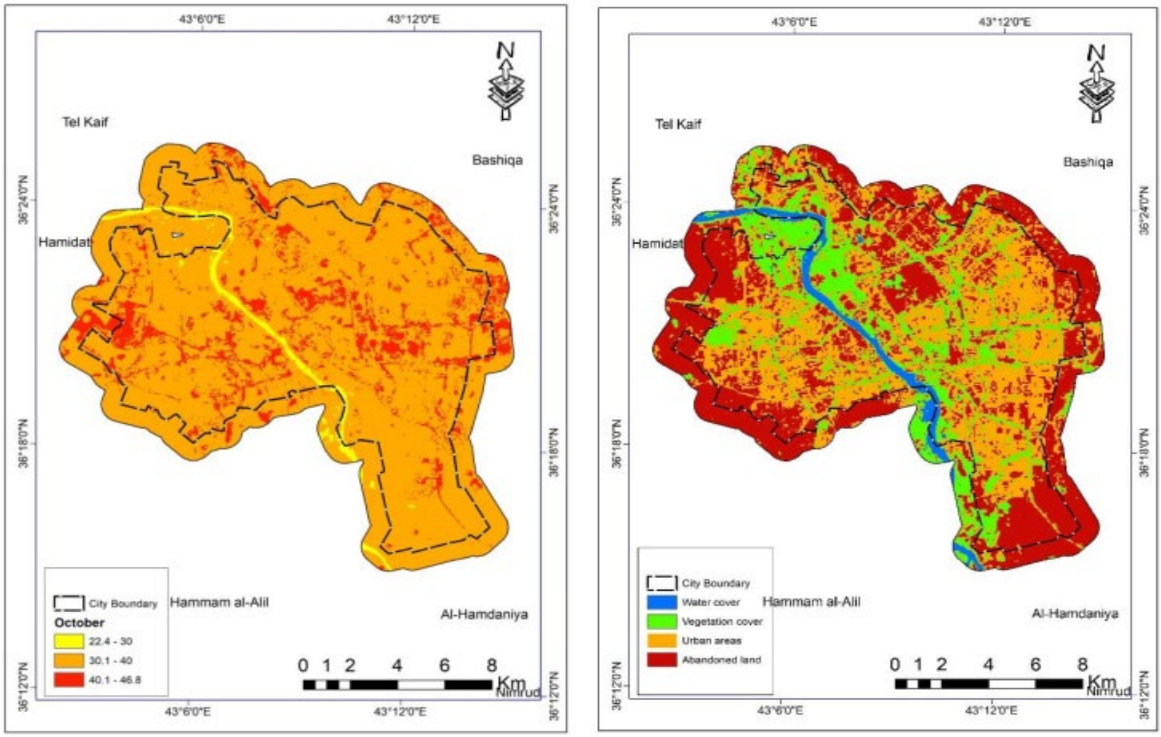

Figure 11. Spatial comparison between ground surface temperature and urban land uses in the city of Mosul during the autumn of 2025

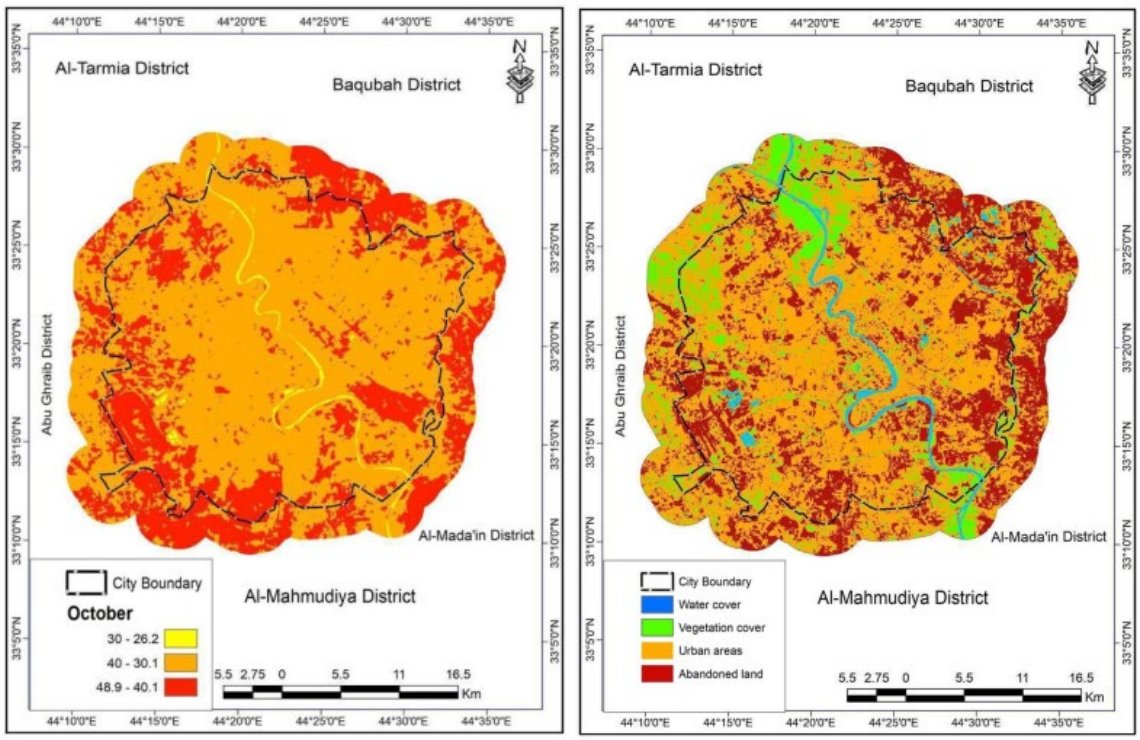

Figure 12. Spatial comparison between ground surface temperature and urban land uses in Baghdad during the autumn of 2025

The percentage of the study area of Mosul that has a temperature higher than 40 ℃ is reduced to about 13.2%, and the temperature class 30.1–40.0 ℃ covers 84.6% of the Mosul area. This is because of the large spatial variability with respect to summer and the quite rapid seasonal transition to lower temperature values. In Baghdad, the surface temperatures also show a decrease in the same manner, but the decrease is not as clear as in Mosul. The 30.1–40.0 ℃ class covers 69.0% of the city's area, whereas the 40.1–48.9 ℃ class accounts for 30.1%. This indicates that a large part of the urban

area maintains high surface temperatures post-summer peak. This pattern might be associated with the thermal effect of urban surfaces and land use properties that generate spatial variations in LST. However, Basra is the city where high temperatures prevail for the longest period, as the class 40.1–50.3 ℃ covers approximately 72.0% of the study area. In comparing spring with autumn, it is evident that the special thermal trait of Basra is not only its ability to reach high temperatures, but to do so for a long time, as areas above 40 °C are still extensive [19].

In general, the results reveal that the main feature of Basra's seasonal thermal regime in 2025 is the persistence of high temperatures compared with Mosul and Baghdad. Mosul shows a relatively rapid autumnal contraction of high-temperature areas, whereas Baghdad represents a transitional case, in which a fairly large area retains high temperatures after summer. This difference further emphasizes the need to consider seasonal persistence, in addition to maximum temperature and spatial extent, when examining SUHI patterns [16].

Table 11. Distribution, area, and percentage of land surface temperature (LST) classes in the study cities during the autumn of 2025

City	Temperature class (℃)	Area (km²)	Percentage (%)
Mosul	22.4–30.0	5	2.2
Mosul	30.1–40.0	193	84.6
Mosul	40.1–46.8	30	13.2
Baghdad	26.2–30.0	12	0.9
Baghdad	30.1–40.0	884	69.0
Baghdad	40.1–48.9	385	30.1
Basra	26.5–30.0	4	2.3
Basra	30.1–40.0	39	25.7
Basra	40.1–50.3	112	72.0

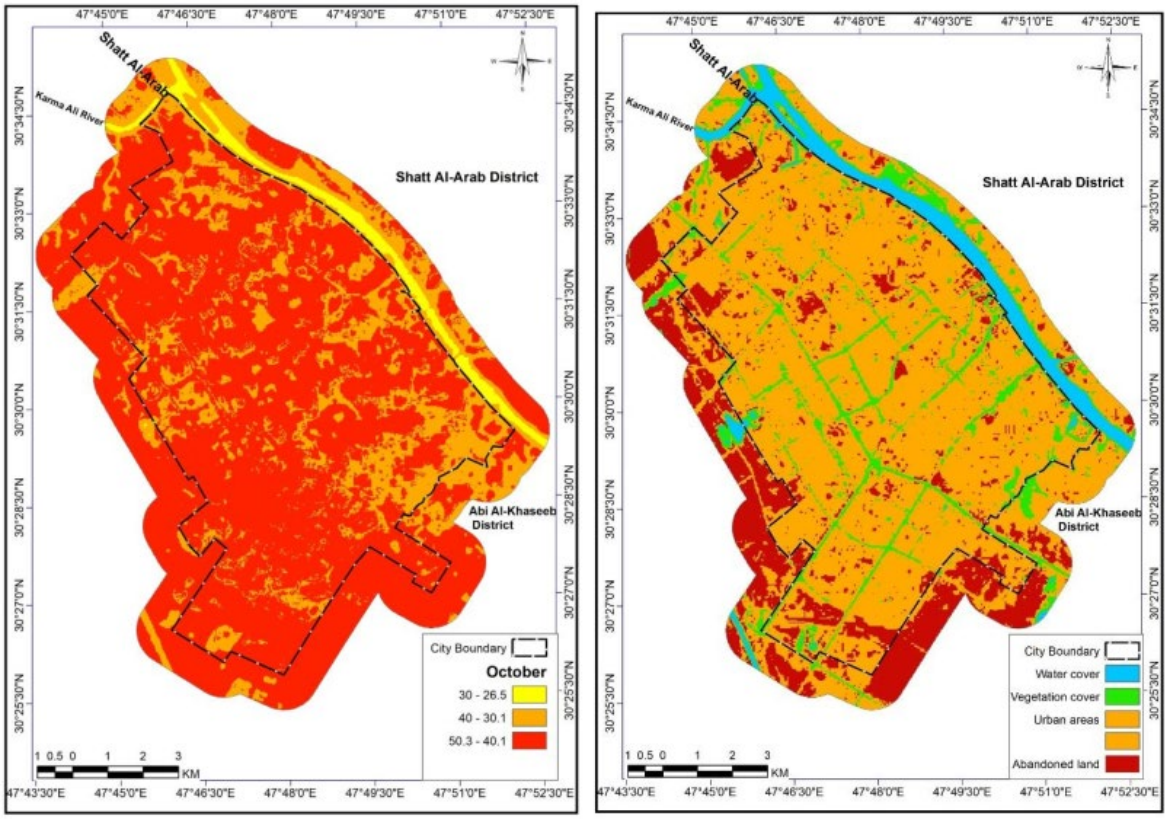

Figure 13. Spatial comparison between ground surface temperature and urban land uses in the city of Basra during the autumn of 2025

4. DISCUSSION

The results indicate that Iraq's climatic gradient provides the general background for the thermal differences between the study cities, but does not alone determine the characteristics of SUHIs. The position of the cities in the ranking changes depending on the season and the indicator used. The maximum LST is highest in Basra in winter, spring, and autumn, whereas Mosul has the highest summer peak (60.9 ℃). The ranking also differs with respect to SUHII: Basra has the highest intensity in winter, Baghdad in spring, and Mosul in summer and autumn. These results confirm that SUHII is not always associated with the maximum absolute LST, since it depends on the LST difference between the urban area and the rural reference zone [5-8]. Thermal differences among the study cities are also related to their urban structure and land cover composition. The main feature of Mosul is its high seasonal thermal peak, partly due to the large proportion of vacant and unused land, which represents about 40.7% of the city's area. The large areas of dry surfaces may lead to faster surface warming, which is consistent with the city's highest summer thermal peak and SUHII. At the same time, vegetation cover and the Tigris River create locally cooler areas, thus breaking the spatial continuity of high temperatures [8, 9, 12]. Baghdad, in contrast, differs from the other cities in the spatial distribution of high-temperature zones rather than

in the highest thermal peak. The upper temperature class covers 62.3% of Baghdad's area, while built-up land accounts for 62.2%. Although these proportions are similar, they do not establish a direct spatial correspondence, as the distribution of elevated temperatures may also be influenced by other land-cover characteristics. Previous studies have also examined the relationships between urban form and thermal conditions, including those reported by studies [13, 20, 21], where the building density and the road density have been positively correlated with the urban heat island intensity, while the green space density has a negative correlation with the urban heat island [22]. Seasonal continuity is the most prominent thermal characteristic of Basra. Approximately 93% of areas experience surface temperatures exceeding 40.1 ℃ in spring and 72% in autumn. This study adopted a thermal threshold of 40.1 ℃ or higher to identify areas with high surface temperatures, serving as an analytical classification boundary to distinguish these high-temperature zones from other thermal categories within the study area. The application of a uniform threshold across the three cities and all four seasons aims to achieve consistency in classification and facilitate spatial comparison of the extent of high-temperature areas. This value does not represent a climatic limit or a general standard for measuring heat stress; rather, it is used for spatial analysis and comparison between cities based on surface temperature data extracted from satellite imagery. This is attributed to the warm climate of southern Iraq, which, at the local level, reduces surface temperature through transpiration and shading [7-10, 21]. The results together show that these study cities are not just different intensities of one thermal pattern, but rather different urban thermal patterns. Mosul has a high summer thermal peak, Baghdad has great spatial coverage of high-temperature areas, and Basra has a high seasonal persistence of high temperatures. Accordingly, the interpretation of SUHIs should not rely on a single variable. Instead, an integrated analytical framework is required that combines maximum temperature, spatial extent, seasonal persistence, and land-cover characteristics, since each indicator reveals a different dimension of the urban thermal structure [4, 5, 9, 14].

The spatial variations in LST observed across the study area are highly aligned with structural and morphological differences in built environment configuration. These thermal patterns can be better understood through the findings of Suleiman and Ali [23], who revealed how structural changes in residential layout and street density govern spatial characteristics in western Iraqi settlements. Moreover, as noted by Abd et al. [24] in their study on urban form in Haditha, the physical imprints of residential developments in arid zones significantly alter surface exposure and thermal retention properties. Consequently, the high proportion of impervious built surfaces and compact residential fabrics continuously influence microclimatic behavior and intensify SUHI effects.

5. CONCLUSIONS

The study concluded that there is a clear spatial and seasonal variation in the characteristics of urban surface heat islands among the cities of Mosul, Baghdad, and Basra during 2025, as well as variations in thermal differences between urban and surrounding rural areas. Mosul experienced the highest peak surface heat during the summer, while Baghdad recorded the widest extent of high summer heat categories, and Basra recorded the highest heat island intensity in winter. These results reflect the different thermal patterns among the three cities and underscore the importance of studying the variation between urban and rural areas in light of climatic and spatial characteristics and land cover composition to understand the thermal distribution of heat islands in Iraqi urban environments.

REFERENCES

[1] Arnfield, A.J. (2003). Two decades of urban climate research: A review of turbulence, exchanges of energy and water, and the urban heat island. International Journal of Climatology, 23(1): 1-26. https://doi.org/10.1002/joc.859

[2] Voogt, J.A., Oke, T.R. (2003). Thermal remote sensing of urban climates. Remote Sensing of Environment, 86(3): 370-384. https://doi.org/10.1016/S0034-4257(03)00079-8

[3] Weng, Q.H. (2009). Thermal infrared remote sensing for urban climate and environmental studies: Methods, applications, and trends. ISPRS Journal of Photogrammetry and Remote Sensing, 64(4): 335-344. https://doi.org/10.1016/j.isprsjprs.2009.03.007

[4] Aya, M.R., Kadhim, A.A. (2025). Land surface temperature estimation from Landsat thermal infrared imagery in Karbala, Iraq. Iraqi National Journal of Earth Sciences, 25(1): 343-353. https://doi.org/10.33899/earth.2024.144879.1179

[5] Zhou, D.C., Xiao, J.F., Bonafoni, S., et al. (2019). Satellite remote sensing of surface urban heat islands: Progress, challenges, and perspectives. Remote Sensing, 11(1): 48. https://doi.org/10.3390/rs11010048

[6] Kim, Y.H., Baik, J.J. (2004). Daily maximum urban heat island intensity in large cities of Korea. Theoretical and Applied Climatology, 79(3-4): 151-164. https://doi.org/10.1007/s00704-004-0070-7

[7] Chow, W.T.L., Roth, M. (2006). Temporal dynamics of the urban heat island of Singapore. International Journal of Climatology, 26(15): 2243-2260. https://doi.org/10.1002/joc.1364

[8] Peng, S.S., Piao, S.L., Ciais, P., et al. (2012). Surface urban heat island across 419 global big cities. Environmental Science & Technology, 46(2): 696-703. https://doi.org/10.1021/es2030438

[9] Emmanuel, R., Fernando, H.J.S. (2007). Urban heat islands in humid and arid climates: Role of urban form and thermal properties in Colombo, Sri Lanka and Phoenix, USA. Climate Research, 34: 241-251. https://doi.org/10.3354/cr00694

[10] Patel, S., Indraganti, M., Jawarneh, R.N. (2024). A comprehensive systematic review: Impact of land use/land cover (LULC) on land surface temperatures (LST) and outdoor thermal comfort. Building and Environment, 249: 111130. https://doi.org/10.1016/j.buildenv.2023.111130

[11] Mallick, J., Rahman, A., Singh, C.K. (2013). Modeling urban heat islands in heterogeneous land surface and its correlation with impervious surface area by using night-time ASTER satellite data in highly urbanizing city, Delhi-India. Advances in Space Research, 52(4): 639-655. https://doi.org/10.1016/j.asr.2013.04.025

[12] Shaltagh, A.G. (2025). The impact of urban land uses on

heat island in Rusafa Municipality (Baghdad) using remote sensing and GIS techniques. Al-Adab Journal, 155 (Supplement): 277-296. https://doi.org/10.31973/fz1szj73

[13] Alshammari, L., Ridha, S., Al-Shammari, M. (2025). Monitoring the urban heat island effect in Baghdad using Sentinel-3 and OSM data integration for sustainable urban planning. Journal of Applied Engineering Science, 23(1): 151-164. https://doi.org/10.5937/jaes0-54589

[14] Wong, N.H., Tan, C.L., Kolokotsa, D.D., Takebayashi, H. (2021). Greenery as a mitigation and adaptation strategy to urban heat. Nature Reviews Earth & Environment, 2(3): 166-181. https://doi.org/10.1038/s43017-020-00129-5

[15] Hammad, N.A., Sbar Hamad, N. (2026). Spatial and temporal changes in vegetation cover in response to extreme climatic phenomena in arid environments: Using remote sensing in Ramadi, Iraq (2024-1980). Pollution, 12(4): 1172-1184.

[16] Mutar, Z.F., Hamad, N.S. (2024). Estimating long-term trends in the elements and some phenomena of Iraq's climate. Dirasat: Human and Social Sciences, 51(5): 33-54. https://doi.org/10.35516/hum.v51i5.10018

[17] Farhan, S.H., Fayyadh, A.F. (2026). Estimation of surface runoff and its utilization potential in Wadi Al-Ghadf basin, western Iraq using the soil conservation service curve number model. International Journal of Design & Nature and Ecodynamics, 21(8): 2429-2438. https://doi.org/10.18280/ijdne.210823

[18] Satam, A.T.M., Aldulaimi, A.M.K., Mushref, Z.J. (2022). Assessment of the water environment of the Euphrates River in the district of Fallujah. AIP Conference Proceedings, 2400(1): 040005. https://doi.org/10.1063/5.0112622

[19] Al-Fahdawi, A.H.A., Satam, A.T.M. (2022). A study of the water reality of managing the Euphrates River in Anbar Governorate in light of the growing water demand for the period (2020-2040). AIP Conference Proceedings, 2400(1): 040004. https://doi.org/10.1063/5.0125471

[20] Satam, A.T.M., Mohammad, E.A., Najm, A.A., Mushref, Z.J., Khalaf, A.M. (2025). Integration of remote sensing, GIS, and SCS-CN model for runoff volume estimation in Al-Deir Valley Basin, Iraqi Jazira Desert. International Journal of Geoinformatics, 21(9): 58-68. https://doi.org/10.52939/ijg.v21i9.4443

[21] Satam, A.T.M., Mekhlef, S.A., Mushref, Z.J., Sulaiman, S.O. (2024). Sustainable management strategies of the water pollution of the Euphrates River within Ramadi City west of Iraq. International Journal of Sustainable Development and Planning, 19(9): 3587-3593. https://doi.org/10.18280/ijsdp.190926

[22] Satam, A.T.M., Mukhlef, W.H., Razzaq, A.S.A.A., Mushref, Z.J., Sulaiman, S.O. (2025). Spatial and temporal variations in water quality of the Euphrates River: A sustainable water management approach for Anbar Governorate, Iraq. International Journal of Design & Nature and Ecodynamics, 20(1): 99-106. https://doi.org/10.18280/ijdne.200111

[23] Suleiman, N.A., Ali, B.B. (2025). Morphological development of the residential unit in the Iraqi City (Fallujah City-Case Study). Dirasat: Human and Social Sciences, 52(6, Supplement 1): 7633. https://doi.org/10.35516/hum.v52i6.7633

[24] Abd, H.Z., Ali, B.B., El Kenawy, A.M. (2026). Housing morphology and urban form in Haditha, western Iraq: Evidence of urban imprints in arid environments. Journal of Asian Architecture and Building Engineering, 1-22. https://doi.org/10.1080/13467581.2026.2746869